Computational stochastic mechanics

S.L. Clemens
Academy of Mathematics, University of Mississippi, USA

E. Garcia & J. Vazquez
University of Barcelona, Spain

ABSTRACT: Model test results show that when raft thickness is 1/6 of column span, the rigidity of frame structure with raft foundation is limited rigidity; and contact pressure of foundation may distribute linearly. The simplified global analysis method with the consideration of superstructure for the contact pressure and settlement of raft under partial load and superimposition principle can be employed in the settlement of large-area thick raft foundation with multi-tall buildings.

Keywords: urban environments, geotechnical engineering, raft thickness, frame structure

1 INTRODUCTION

Large number of sites underlain by soft peaty clays are now being used for various constructions due to the scarcity of land. These are used for the construction of buildings as well as for the development of new infrastructure facilities such as highways. Soft peaty clays are of very low shear strength and are extremely compressible due to their very high water contents and void ratios. Constructions done on peaty clays could be subjected to very large settlements due to their high compressibility. Catastrophic failures are also possible due to very low shear strength. Problems due to these characteristics can be overcome by either transferring the loads to harder strata underneath through piles or by improving the engineering properties of Peat to a desired level.

Use of a fill material of lower density is another possible approach that can be adopted in some constructions done on soft peaty clays. This would be particularly useful in the construction of embankments (Clarken, 1986) Lightweight fill materials impose lower loads on the underlying soft soils resulting in lower settlements and reducing the possibilities of shear failure. Lightweight fill materials such as polystyrene blocks were used successfully in countries like U.K in construction over soft soils. However, it is not economical to import such material to the country. To provide an economical solutions lightweight fill materials should be developed locally.

As such, attempts were made at University of Moratuwa to develop lightweight fills by mixing different proportions of tyre chips with lateritic soil, sawdust with lateritic soil and paddy husk with lateritic soil. Tyre chips were obtained by shredding the discarded motorcar tyres. Sawdust is obtained from wood mill waste and paddy husk is obtained from rice mill waste. The developed material should be sufficiently incompressible and should possess adequate shear strength. Further detailed tests were conducted on selected mixes to establish their engineering characteristics in relation to strength and stiffness. The criterion to be achieved is that the in-service settlement should be less than 50mm.

2 PILE TEST METHOD FEATURES BY DYNAMIC LOADING

The using of the pile foundation is accompanied by the demand of the determination of the pile load bearing capacity according to the results of its field tests under the sustained dynamic load. The procedure of such tests is stated in (2) and its gist is in the formation and the using of the «load-pile settlement» dependence, which is received experimentally, moreover the last includes the settlement created owing to the sustained vibration besides the statical settlement. Evidently that this procedure of the experimental data processing can not be enough accurate since it is based on the just a second result and does not take into account in the first place the time factor. For the examination of problem about the pile load bearing capacity, subjected to the sustained vibration load action the static dynamic tests of 15 driven reinforced concrete piles C 14-35 beared against the sandy soils were carried out.

The test realization procedure is in accordance with the demands of the Supplement 2 (2); the dynamic stage was carried out on the operating fre-

quency of the low speed turbo-generator set at 25 Hz with the amplitude vertical oscillations of 10 mkm. The experimental data processing was carried out by two ways : according to (2) and according to the ways described below. The test results are given in the table 1.

Table 1. The pile test data by the sustained dynamic loads

№ of pile	Special value of the limiting resistance, F_u, kN	General dynamic stage time, t, hour.	The stage time to the point of the conditional stabilization reaching: t, hour
Site 1			
C-4	750	70	-
C-6	800	-	-
C-8	1200	70	50
C-10	1000	35	20
C-12	800	85	-
C-16	800	85	-
C-21	1200	100	40
Site 2			
C-6	800	106	-
C-8	1100	93	-
C-9	850	66	30-
C-11	1000	78	30
C-27	900	35	-

3 WATER PRESSURE IN THE FOUNDATION

A significant concern on the safety of arch dams is the uplifting force of water pressure below the foundation. Scour processes in joints below the dam may change the flow behaviour. The issue can easily be assessed by the evaluation of piezometer heads in the foundation.

It is most satisfying that four out of five installed piezometers are still operational. The piezometers read the water pressure below the dam foundation that is equivalent to the uplift.

PZ02 (+2.0 masl) is installed in the right abutment and 5 m below the dam foundation. This is equivalent to 32 m below retention water level. PZ10 (+10.0 masl) is installed in the left abutment 5 m below the dam foundation. The difference to the retention water level is 24 m. PZ04 (-9.0 masl) is installed in between the centre of the dam and the right abutment 5 m below the dam foundation. The difference to the retention water level is 43 m. PZ06 (-14.5 masl) is 10 m below the dam foundation installed in its centre. The difference to the retention water level is 48.5 m.

Figure 1 shows the readings of the four operational piezometers since implementation of the dam. Mostly, their pressure level agrees with their installation depth below water table. PZ06 shows highest values. Seasonal variations correspond to the variations in water table.

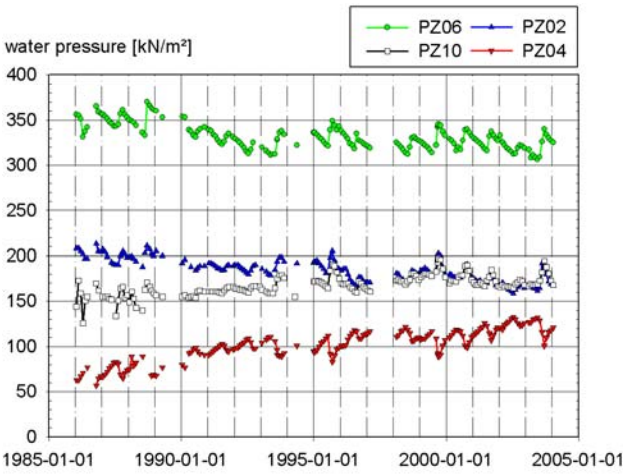

Figure 1. Piezometer readings since implementation

PZ04 shows the lowest pressures, were higher values were expected. It is supposed that the high potential decrease occurs upstream of PZ04. While the three other piezometers showed an almost constant or decreasing piezometer head, pressure in PZ04 increases slowly since implementation time. The increase is most probably due to transportation of fines in joints. However, a regression analysis by the Consultant confirmed that the gradient is decreasing. An extrapolation to 2008 showed that a constant value slightly above of 120 kN/m².

The Consultant conducted a safety analyses that proved that none of the piezometers has reached critical uplift values. Until today the dam foundation is safe and sound.

4 GEOTECHNICAL MODEL

Several geotechnical models were formulated to represent the variable subsurface conditions along the alignment. The models were derived from the results of vane shear testing (which was conducted within boreholes at 1m depth intervals) and piezocone test results. Over the majority of the east bund alignment, where the clay thickness was between 25m and 30m, a single model was adopted with the shear strength being a constant 5kPa to 3m depth below the seabed increasing thereafter at a rate of 1.5kPa/m depth i.e. 0.25 x effective vertical stress. This is illustrated in Figure 2. It was also recognised that, based on the available shear strength data, lower shear strength profiles could exist locally along the alignment. The lower bound profiles were used for sensitivity analyses.

Concerns were raised regarding construction activities including geotextile placement, layer thickness to minimize mudwaving, turbidity conditions, toe heaving and mud waving. It was therefore agreed to construct instrumented trial embankments to obtain a better understanding and provide confidence in the design and construction phases. Several issues

were important geotechnically, including construction procedures and loads for stability analyses, design parameters related to initial deformation and the ability to place geotextiles under water without folding (which would result in loss of load capacity).
Two trials were conducted: one inshore using land-based equipment; and the other offshore using marine based floating plant. Details of these trials are presented by Ameratunga et al (2003) and a summary is given below.

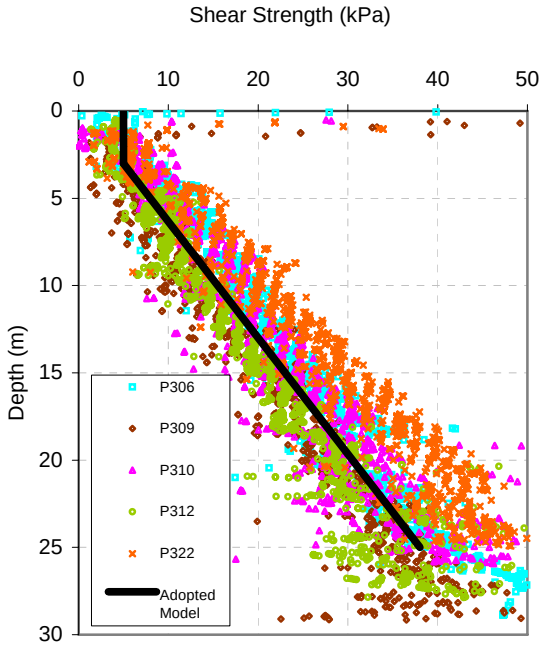

Figure 2. Shear strength profiles of a few piezocones on the east bund

The land based trial comprised 3 x 20m sections of a multi-level rock bund up to 3m high with one of the bunds placed on a high strength geotextile whilst the others were placed directly on the seabed. The marine based trial had two separate bunds with one bund consisting of a 2m core rock layer on a geotextile and the other consisting of a 2m sand layer directly on the seabed with 1.5m of rock core on top. Ameratunga et al (2003) describe the geotechnical models adopted and analyses conducted using commercially available software PLAXIS and FLEA.

The trials provided valuable data which were used for back analyses. As a result, elastic deformation parameters for the soft clay under the east bund was modified and a value of 100 was adopted for the ratio of undrained Young's modulus and undrained shear strength. The trial results highlighted potential conservatism in the treatment of construction equipment loads and geometry in stability analyses in the direction of the alignment because of three dimensional effects.

Another concern was the expected damage to the geotextile due to rock placement and trafficking. While empirical equations were available for geofabric strength assessment due to falling rock, no literature could be found on trafficking. Several panels were constructed on land and rocks of different but known sizes were dropped at different heights. Panels were separately subjected to trafficking to assess damage. Damage on each panel was quantified and a damage factor of 1.7 was adopted to downrate the geotextile strength.

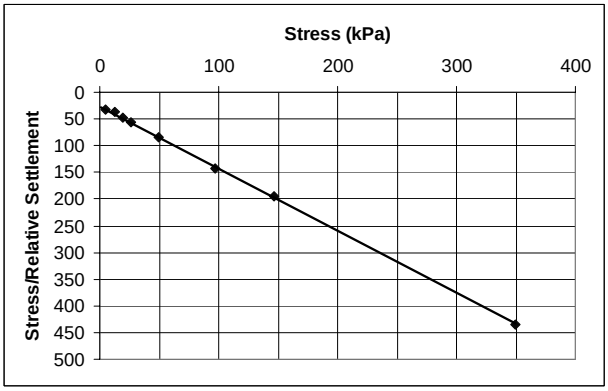

Figure 3. Stress to strain ratio as function of stress for the dry test

4.1 *Hyperbolic Model for MSW immediate settlements*

In a first approach, the data were modeled using different mathematical functions. When the data were plotted as stress divided by strain versus the stress (or a hyperbolic-type curve), a strong linear relationship was observed. This was not a surprise since the two variables plotted (x and y axes) are not independent, but help in the study of the significance of the parameters of the curve, as will be shown further. Figure 3 presents the graph of stress-to-strain ratio as a function of stress for the dry test. The results for other tests follow similar patterns.

The same procedure was applied to other data published in the general literature. The studies of Debnath (2000) and Carvalho (1999) were added to the present study to understand the immediate settlement mechanism of MSW. Both studies utilized compression chambers to study the MSW compressibility. In all cases, the stress-to-strain ratios as functions of stress were straight lines. Therefore, it is reasonable to conclude that the MSW immediate settlement can be expressed as:

$$\frac{\sigma_v}{\varepsilon} = a \cdot \sigma_v + b \qquad (1)$$

where σ_v is the total vertical stress at the middle of the layer , ε is the strain and a and b are the constants of the linear curve. Since the strain can be written as the ratio between the settlement and the initial thickness of the layer, Equation 1 can be expressed as:

$$\Delta H_i = \frac{\sigma_v \cdot H_0}{a \cdot \sigma_v + b} \quad (2)$$

where ΔH_i is the immediate settlement and Ho is the initial thickness layer (assuming the stress at the middle of waste layer equal to zero).
If the initial thickness under compression and initial stress are taken into account, Equation 2 can be represented by a more specific expression, as shown in Equation 3.

$$\Delta H_i = \frac{H_e \cdot \sigma_v \cdot (a \cdot \sigma_{ve} + b)}{[(a-1) \cdot \sigma_{ve} + b)] \cdot (a \cdot \sigma_v + b)} - \frac{\sigma_{ve} \cdot H_e}{(a-1) \cdot \sigma_{ve} + b} \quad (3)$$

where σ_{ve} is the initial stress at the middle of the waste layer before compression and H_e is the respective initial thickness of the waste layer before compression.

4.2 *Calibration of model parameters*

Constitutive parameters for the sand were obtained by performing a Class C analysis of a centrifuge test of an instrumented level sand bed of the same density as that used in this study. The model parameters were varied to achieve a best fit to the pore-pressures and accelerations measured within the sand bed. These histories show the excess pore-pressures close to the end wall of the model container and at the centre of the bed at 12m depth. In both cases, a very good match was achieved between centrifuge test data and FE results.

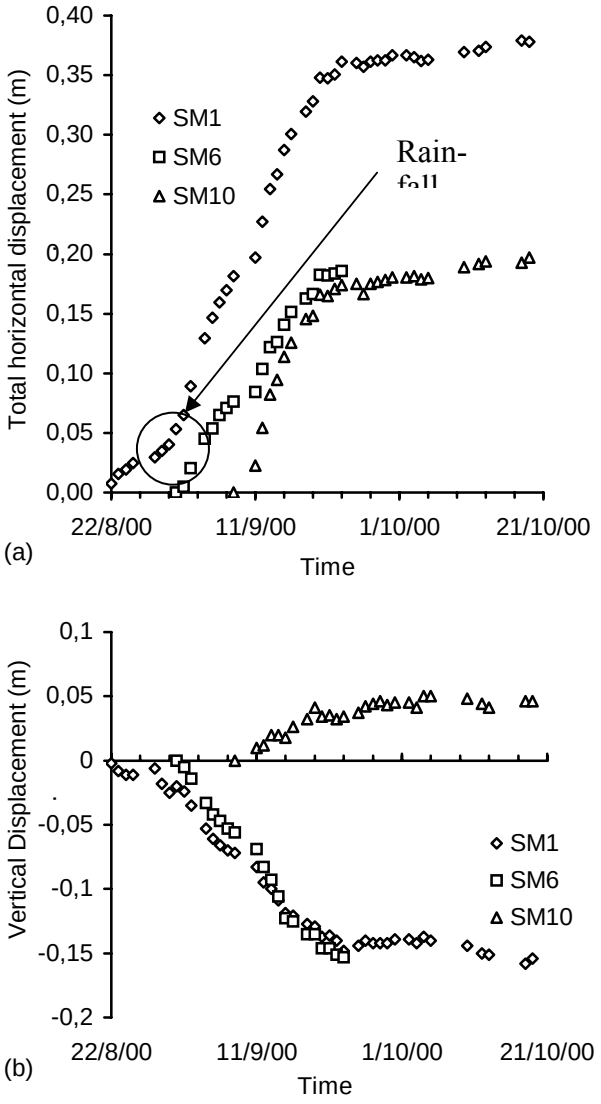

Figure 4. a) Magnitude of movements on the horizontal plane, and b) on the vertical plane (positive outwards and upwards respectively).

5 FINAL STABILIZATION MEASURES

Geological and geotechnical investigation that followed movement initiation revealed that despite the favourable dip direction of flysch layers relative to the slope of the excavation face, the very poor engineering properties of the flysch, especially at the toe of the excavation, were inadequate to ensure the stability of the cut. Inclination of movements on the surface monuments at the toe coincided with the dip of the flysch layers (20^o). Additionally, faults of opposite dip direction at the scarp allowed the creation of a rather unusual failure mechanism which, in combination with temporary perched water tables initiated by heavy rainfall, resulted in instability.

In order for the temporary cut's factor of safety to reach an acceptable level for the construction of the twin concrete tunnels, support measures in addition to the unloading excavation included decrease of the slope to 1 over 1.5 (vertical over horizontal) and three rows of prestressed anchors. The upper two had 25m long anchors at 2m spacings and the lower one 35m long anchors at 2m spacing. Such lengths were required in order for the fixed length of the anchors to lie certainly beyond the failure surface. Locally placed horizontal drainage holes (a total of 25 20m holes were drilled) were also placed in order to cope with possible new perched water tables. After the implementation of these additional support measures, construction of the twin concrete tunnels and placement of fill on top of them continued as initially designed.

The static axial load (P_{static}) acting in the building is reported to be 416kN. Input motion measured in the nearby Higashi-Kobe Bridge showed a peak ground acceleration of 0.38g. However, the PGA at the building site is not known. The piles used in the building had an external dia. (D_O) of 0.4m and inside dia. (D_i) of 0.24m. A preliminary analysis incorporating the SPT values and Z_{WT} in the random vector revealed that the p_F for this type of structure is insensitive to these variables. The soil profile and the water table is taken as deterministic and thus not included as a variable. Thus there are altogether nine variables in the analysis, which are uncertain and therefore treated as random. Because the probability

distributions and co-variances of these variables are not known, it is assumed that they are normally distributed and uncorrelated. Further due to non-availability of the relevant data, a uniform coefficient of variation of 0.1 has been assumed for all the variables.

It may be noted that the outside diameter has the highest value of importance factor. It was therefore agreed to construct instrumented trial embankments to obtain a better understanding and provide confidence in the design and construction phases. Several issues were important geotechnically, including construction procedures and loads for stability analyses, design parameters related to initial deformation and the ability to place geotextiles under water without folding

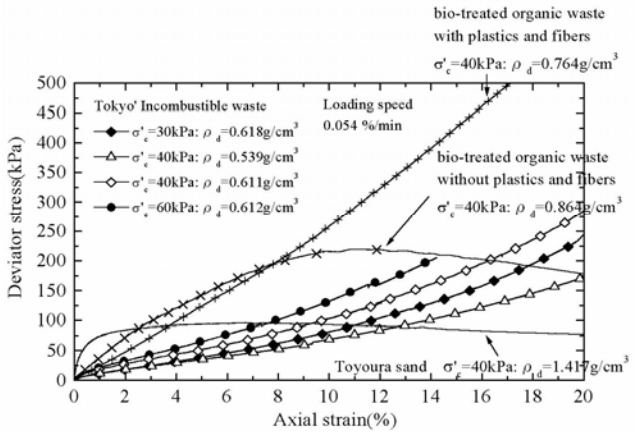

Figure 5. Stress-strain relationship of incombustible waste.

6 TRANSFER FUNCTIONS

Considering vertically propagating waves and linear histeretic soil behavior, the resulting transfer function, surface to bedrock, is only a function of the soil properties and thickness of the soil layers, and therefore, it represents the site effect, regardless the characteristics of the shaking (Roesset 1977; Roesset et al, 1969; Kramer, 1996). However, it is important to bear in mind that shear modulus and damping ratio are strain dependent, and therefore, controlled by the shake intensity, which means that the transfer function should be also dependent on the level of the seismic event. Nevertheless, the available data represent small earthquakes where the non-linearity of the soil behavior should not appear.

Because response spectra are less sensitive to noise and peaks are easier to be identified, the transfer functions between surface and bedrock were computed using the ratio of the velocity response spectra instead of the Fourier transform. The average transfer function for the N-S and E-W components obtained from 11 recorded earthquakes is presented in Fig. 5. On the other hand, from a theoretical analysis for vertically propagating shear waves assuming linear elastic soil behavior for the soil properties shown in Figs. 2, the first natural period in shear has a value of T_{s1} = 0.74 sec and the second a value of T_{s2} = 0.27 sec.

7 TRIAXIAL SHEAR TESTS

Conventional triaxial drained compression tests were conducted to study the stress-strain-strength properties of wastes.

7.1 *Incombustible waste*

7.1.1 *Test results*

The results of triaxial shear tests on incombustible as well as biotreated wastes are shown in Fig.6. It is seen therein that the strength and rigidity increase with the density of sand. More over, the material strength increases with the confining pressure. These findings are consistent with the behavior of soils. As compared with Toyoura sand data, the initial rigidity of waste is smaller, while the strength of waste at large strain is much greater, without yielding. This nonyielding behavior was generated by plastic and other fibrous inclusions, which is evidenced by the fact that the biotreated waste (Towhata et al., 2003) with big fibers removed exhibits yielding at 10% strain. This reinforcing effects of fibers do not occur in rigidity because fibers do not yet undergo sufficient tension. Finally, Mohr stress circles were drawn at 15% axial strain to demonstrate the internal friction angle increases with compaction.

7.1.2 *Cement mixing*

Fig. 5 shows the stress-strain relation are bio-treated waste of cement-mixed incombustible waste to which geo10 has been added. For 60 g of waste material the amount of cement added was 180 g for W/C=0.5 and 105 g for W/C=1.0, thus the void was filled with grout. The strength of the improved sample was found to be higher when W/C of the added cement was smaller. At W/C below 0.8, in most of the improved samples, peak strength occurred and high levels of strength were achieved. For W/C=1.0, strength was still high compared with unimproved specimens, but peak strength did not occur. However, because it is characteristic of unimproved incombustible waste that it tends not to collapse under increased strain, one of the properties of the ground is that it does not collapse.

8 DISCUSSION

In the above two sections, the likelihood of liquefaction occurring after successive earthquakes is shown on two dynamic centrifuge tests. The first test has four successive earthquakes applied to the same soil model and liquefaction ratios decrease proving the

re-liquefaction to depend on the intensity of each earthquake and the change in the loose structure of the soil as it densifies with each earthquake. The second example has shown the use of CPT testing to assess changes in density of the soil structure and hence to assess the liquefaction susceptibility after successive earthquakes. It is seen that with successive earthquakes the possibility of liquefaction reduces and the values approach the boundary between liquefaction and non-liquefaction zones.

9 CONCLUSIONS

A series of dynamic loading tests was performed to investigate dynamic responses of soil and liquefaction behavior under various loading types. Based on test results, detailed dynamic responses of soils, including mobilization of excess pore water pressure, deviatoric stress, and effective stress path under regular and irregular real earthquake motions were compared and analyzed. Stress damage concept based on the stress-time history and the cumulative energy obtained from the stress-strain curves were also introduced and investigated for different types of dynamic loadings.

From the test results, it was found that cyclic loading tests with sinusoidal and triangular signal do not accurately simulate dynamic responses of soil under real earthquake loadings. From results of mobilization of excess pore water pressure and initial liquefaction, a new classification of earthquake motions into blazing and terraced types was proposed. For the blazing type, the initial liquefaction occurs near the maximum peak load. For the terraced type, on the other hand, subsequent loadings of high amplitudes after the maximum peak loading point were also important consideration for the initiation of liquefaction.

From the investigation of the cumulative energy and stress damage ratio, it is confirmed that the use of the cyclic loading for seismic analyses may not be effective and likely to result in overestimated input motions. The dynamic loading tests with incremental loading shapes were observed to reflect relatively well the effect of real earthquake loading shape compared to sinusoidal loadings.

ACKNOWLEDGEMENT

The authors are grateful to Mr. G. García Marquez. for providing the information of the historical point of view.

REFERENCES

Daniel, D.E., Shan, H.-Y., and Anderson, J.D. 1993. Effects of partial wetting on the performance of the bentonite component of a geosynthetic clay liner, Geosynthetics'93, IFAI, pp. 1482-1496.

Der Kiureghian, A., Madanat, S. and Pestana, J.M. 2003. Applications of Statistics and Probability in Civil Engineering. Proceedings of the 9th International Conference on Applications of Statistics and Probability in Civil Engineering, San Francisco, California, USA, July 6-9. Rotterdam: Millpress.

Giroud, J.P., Badu-Tweneboah, K., and Soderman, K.L. 1997. Comparison of leachate flow through compacted clay liners and geosynthetic clay liners in landfill liner systems, Geosynthetics International, Vol. 4, Nos. 3-4, pp. 391-431.

Jo, H.Y., Katsumi, T., Benson, C.H., and Edil, T.B. 2001. Hydraulic conductivity and swelling of non-prehydrated GCLs permeated with single species salt solutions, Journal of Geotechnical and Geoenvironmental Engineering, ASCE, Vol.127, No.7, pp.557-567.

Katsumi, T., Onikata, M., Hasegawa, S., Lin, L., Kondo, M., and Kamon, M. 2001. Chemical compatibility of modified bentonite permeated with inorganic solutions, Geoenvironmental Engineering, R.N. Yong and H.R. Thomas (eds.), Thomas Telford, pp. 419-424.

Katsumi, T., Ogawa, A., and Fukagawa, R. 2004a. Effect of chemical solutions on hydraulic barrier performance of clay geosynthetic barriers, Proceedings of the Third European Geosynthetics Conference, pp. 701-706.

Katsumi, T., Ogawa, A., and Fukagawa, R. 2004b. Effect of prehydration on hydraulic performance of geosynthetic clay liners permeated with inorganic chemical solutions, Proceedings of the Third Asian Regional Conference on Geosynthetics, pp. 937-944.

Kolstad, D.C., Benson, C.H., and Edil, T.B. 2004. Hydraulic conductivity and swell of nonprehydrated geosynthetic clay liners permeated with multispecies inorganic solutions, Journal of Geotechnical and Geoenvironmental Engineering, ASCE, Vol.130, No.12, pp.1236-1249.